IOP Publishing Nanotechnology

Nanotechnology 33 (2022) 495705 (7pp)

https://doi.org/10.1088/1361-6528/ac8f51

Study of carbon nanotube embedded honey as a resistive switching material

Md Mehedi Hasan Tanim¹, Brandon Sueoka¹, Zhigang Xiao², Kuan Yew Cheong^{3,*} and Feng Zhao^{1,*}

E-mail: srcheong@usm.my and feng.zhao@wsu.edu

Received 17 June 2022, revised 30 August 2022 Accepted for publication 4 September 2022 Published 20 September 2022



Abstract

In this paper, natural organic honey embedded with carbon nanotubes (CNTs) was studied as a resistive switching material for biodegradable nonvolatile memory in emerging neuromorphic systems. CNTs were dispersed in a honey-water solution with the concentration of 0.2 wt% CNT and 30 wt% honey. The final honey-CNT-water mixture was spin-coated and dried into a thin film sandwiched in between Cu bottom electrode and Al top electrode to form a honey-CNT based resistive switching memory (RSM). Surface morphology, electrical characteristics and current conduction mechanism were investigated. The results show that although CNTs formed agglomerations in the dried honey-CNT film, both switching speed and the stability in SET and RESET process of honey-CNT RSM were improved. The mechanism of current conduction in CNT is governed by Ohm's law in low-resistance state and the low-voltage range in high-resistance state, but transits to the space charge limited conduction at high voltages approaching the SET voltage.

Keywords: honey, carbon nanotube, resistive switching, nonvolatile memory, biodegradable, neuromorphic system

(Some figures may appear in colour only in the online journal)

Introduction

Advancements in information technology, Internet of Things (IoT), artificial intelligence, etc. increase the needs of energy-efficient computing systems. Conventional von Neumann architecture is reaching its bottleneck, and brain-inspired neuromorphic computing has attracted significant interests due to its high energy efficiency and low power consumption [1, 2]. Resistive switching memory (RSM) is one of the promising technologies for nonvolatile random access memory (RAM), the essential data storage device in neuromorphic systems and artificial intelligence. RSM devices have been explored for applications [3, 4] such as nonvolatile static

RAM (nvSRAM) memory cells [5], electronic bio-inspired artificial receptor in neurorobotic technology [6], artificial neural networks [7, 8], logic computing [9], radiofrequency (RF) switch [10], etc. Recently, natural organic materials such as polypeptides (proteins) [11–13] and polysaccharides (carbohydrates) [14–16] have been explored for renewable and biodegradable RSMs with sustainability and minimal electronic-waste due to their unique merits of low cost, ease of processing, bio-resorbable, abundant in nature, and environmental friendliness. As a carbohydrate mixture, natural honey has been reported [17–20] as an encouraging resistive switching material for RSM. Honey is a mixture containing more than 180 constituents [21], mainly sugar, which is represented by about 75% monosaccharides, mainly glucose and fructose, followed by 10%–15% disaccharides such as

¹ Micro/Nanoelectronics and Energy Laboratory, School of Engineering and Computer Science, Washington State University, Vancouver, WA 98686, United States of America

² Department of Electrical Engineering, Alabama A&M University, Normal, AL 35762, United States of America

³ School of Materials and Mineral Resources Engineering, Engineering Campus, Universiti Sains Malaysia, 14300 Nibong Tebal, Penang, Malaysia

^{*} Authors to whom any correspondence should be addressed.

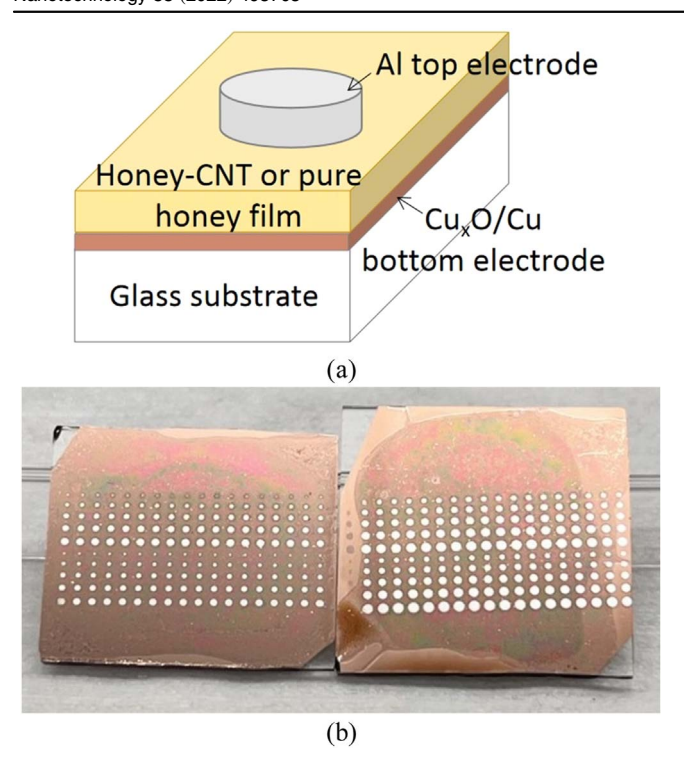


Figure 1. (a) Schematic structure and (b) photographs of honey (left) and honey-CNT (right) RSMs.

sucrose, maltose, turanose, isomaltose, etc, and small amount of trisaccharides of maltotriose and melezitose.

Investigations have been carried out to further improve switching properties of natural organic materials by incorporating carbon-based nanomaterials such as graphene in chitosan [22], graphite nanosheet in keratin [23], and carbon nanotube (CNT) in egg albumen [24]. The improvement by these nanomaterials is attributed to the regulation of formation and rupture of conductive filaments [25]. In this paper, CNT embedded honey as a resistive switching material was studied for the first time.

Experimental

Two 30 wt% honey solutions were prepared by dissolving commercial honey (100%, US Grade A) in D.I. water at room temperature till no visible honey crystals. Next, as-received single wall CNT powders (P0286 HiPco SWCNTs, Carbon Nanotechnologies Inc.) with a 0.2 wt% concentration was dispersed in one honey solution in an ultrasonic bath for 60 min to form honey-CNT solution. Two glass slides $(2.5 \text{ cm} \times 2.5 \text{ cm})$ were cleaned by acetone, IPA and D.I. water, followed by a 100 nm thick Cu film deposition in a Kurt J. Lesker Nano 36 DC/RF sputter system. After deposition, pure honey solution and honey-CNT solution was spin-coated on each slide at 3000 rpm for 60 s. Both samples were baked in an oven at 90 °C for 8 h to form dried honey and honey-CNT thin films. Finally, both samples were deposited a 100 nm thick Al film through a stencil mask as top electrodes with the diameters of 100 μ m, 200 μ m, $300~\mu m$, $400~\mu m$ and $500~\mu m$ to complete the fabrication. Schematic structure and photographs of the RSM devices are shown in figure 1. It is not distinguishable between pure honey and honey-CNT film in photographic pictures.

Surface morphology of the dried honey and honey-CNT films was inspected by a *Wyko NT1100* optical surface profiler and a Nanosurf Flex-Axiom AFM. Resistive switching properties were characterized with the samples on a Signatone probe-station by a Kiethley 4200 semiconductor characterization system in air and at room temperature. RSM devices with the diameter of 100 $\mu \rm m$ on both samples were tested and compared in this study. During all measurements, voltage bias was applied on the Al top electrode while the Cu bottom electrode remained grounded.

Results and discussion

Surface morphologies of the dried honey and honey-CNT films are shown in figure 2. Although honey has a high sugar concentration and therefore tends to crystalize, a long mixing time in D.I. water ensured a complete dissolution of honey in water and no honey crystal in both dried films. The pure honey film is uniform and homogenous as shown in figures 2(a), (b) with an average surface roughness of $0.10 \ \mu m$ across a 1.9 mm \times 2.5 mm area. This roughness was improved from previously reported honey film spin-coated at 1000 rpm and dried at 90 °C for 9 h, which was 0.46 μ m [17]. Although CNT was dispersed in honey-water solution by ultrasonic for 1 h, dispersion was not as effective as in solvent such as ethanol. Entanglement or bundling of CNTs due to strong van der waals force formed a large amount of agglomerations in the honey-CNT film, as shown in figures 2(c), (d). The average roughness of the honey-CNT film across a 0.45 mm \times 0.59 mm area is measured to be 0.14 μ m.

Typical current–voltage (I–V) characteristics of honey and honey-CNT RSM are shown in figure 3(a). Both devices exhibited bipolar resistive switching characteristics without initial forming process. RSM transits from high resistance state (HRS) to low resistance state (LRS) at the SET voltage ($V_{\rm set}$), i.e. the 'writing process', and from LRS to HRS at the RESET voltage ($V_{\rm reset}$), i.e. the 'erasing process'. The current compliance $I_{\rm CC}$ in SET process was 10 mA to prevent dielectric breakdown of the honey and honey-CNT films. Figure 3(a) shows that the honey-CNT film has a lower leakage current and higher ON/OFF current ratio at the read voltage of 0.5 V, although the effect is not as efficient as other nanomaterials in natural organic films, such as CNT embedded egg albumen [24] and gold nanoparticles embedded silkworm hemolymph [26].

Endurance tests were carried out by repeating the switching cycles in figure 3(a) for 200 times. $V_{\rm set}$ and $V_{\rm reset}$ values from each cycle were recorded in cumulative probability plots and shown in figure 3(b). The average and standard deviation of $V_{\rm set}$ and $V_{\rm reset}$ values were 4.1 \pm 2.5 V and -1.83 ± 1.21 V for honey RSM, and 3.56 ± 1.3 V and -1.80 ± 0.63 V for honey-CNT RSM. The coefficients of

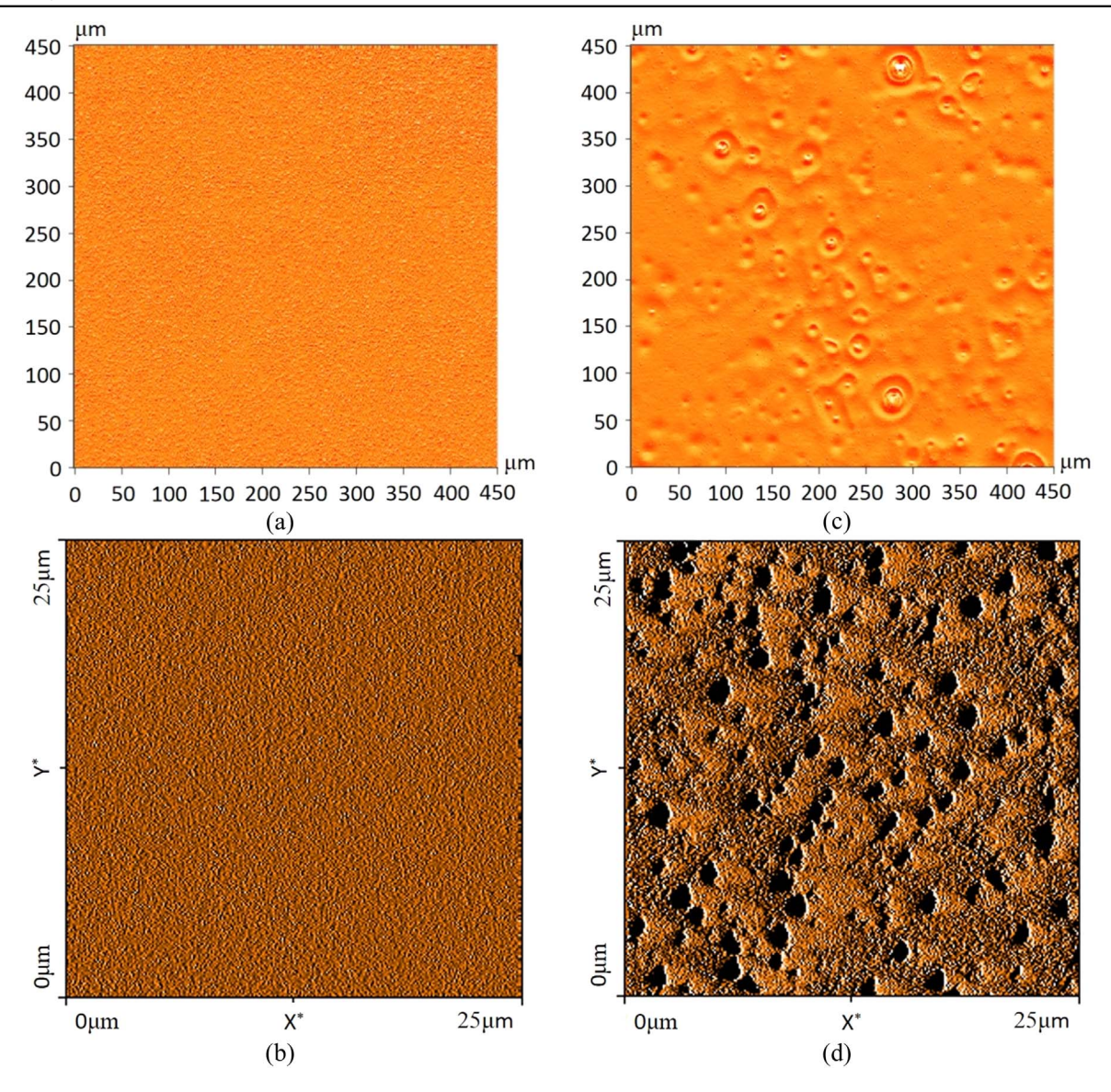


Figure 2. Optical surface profiler and AFM tapping mode images of (a), (b) pure honey film and (c), (d) honey-CNT film.

variation can be calculated by the ratio of standard deviation to average value. They were 0.6 versus 0.36 in $V_{\rm set}$ and 0.66 versue 0.35 in V_{reset} for pure honey and honey-CNT RSM, respectively, with the smaller value indicating a higher stability. CNT in honey improved the stability of V_{set} by 40% and V_{reset} by 47%. This improvement is more efficient than in natural silkworm hemolymph film embedded with gold nanoparticles [26], in which the stability of V_{set} was improved by 3.4% and V_{reset} by 26.4%, respectively. These results proved that CNT embedded honey film can potentially improve the stability of memory device in its 'write' and 'erase' processes. As indicated in figure 2(d), bundles of CNT were dispersed over the honey film which may promote the alignment of conductive filaments formation during 'write' process. CNT is having abundant of surface charges that can be used as a bridge to connect the conductive filaments. During 'erase' process, disconnection of the conductive filaments is attributed to the removal of CNT.

To identify the current conduction mechanism, the I-V curves of honey and honey-CNT RSMs in the forward bias regions in figure 3(a) were replotted in double-logarithm scales, as shown in figure 4(a). All currents of pure honey film in both LRS and HRS and honey-CNT film in LRS showed slopes closed to unity. Such linear relationships indicated that the conduction mechanism is governed by Ohm's law with the resistance of filamentary conductive paths between the top and bottom electrode within the honey and honey-CNT film due to the electrochemical redox of the top Al electrode [17] Positively charged Al ions from top electrode is drifted to bottom electrode and reduced to metal Al [as Al⁰ in figure 4(b)]. The extension of the reduced Al metal stacked from the bottom electrode towards the top electrode is due to the increment of applied voltage. As it approached V_{set} , a larger number of electrons can be transferred from the bottom electrode to the top electrode [figure 4(c)]. An instantaneous surge in current is observed when the full connection of

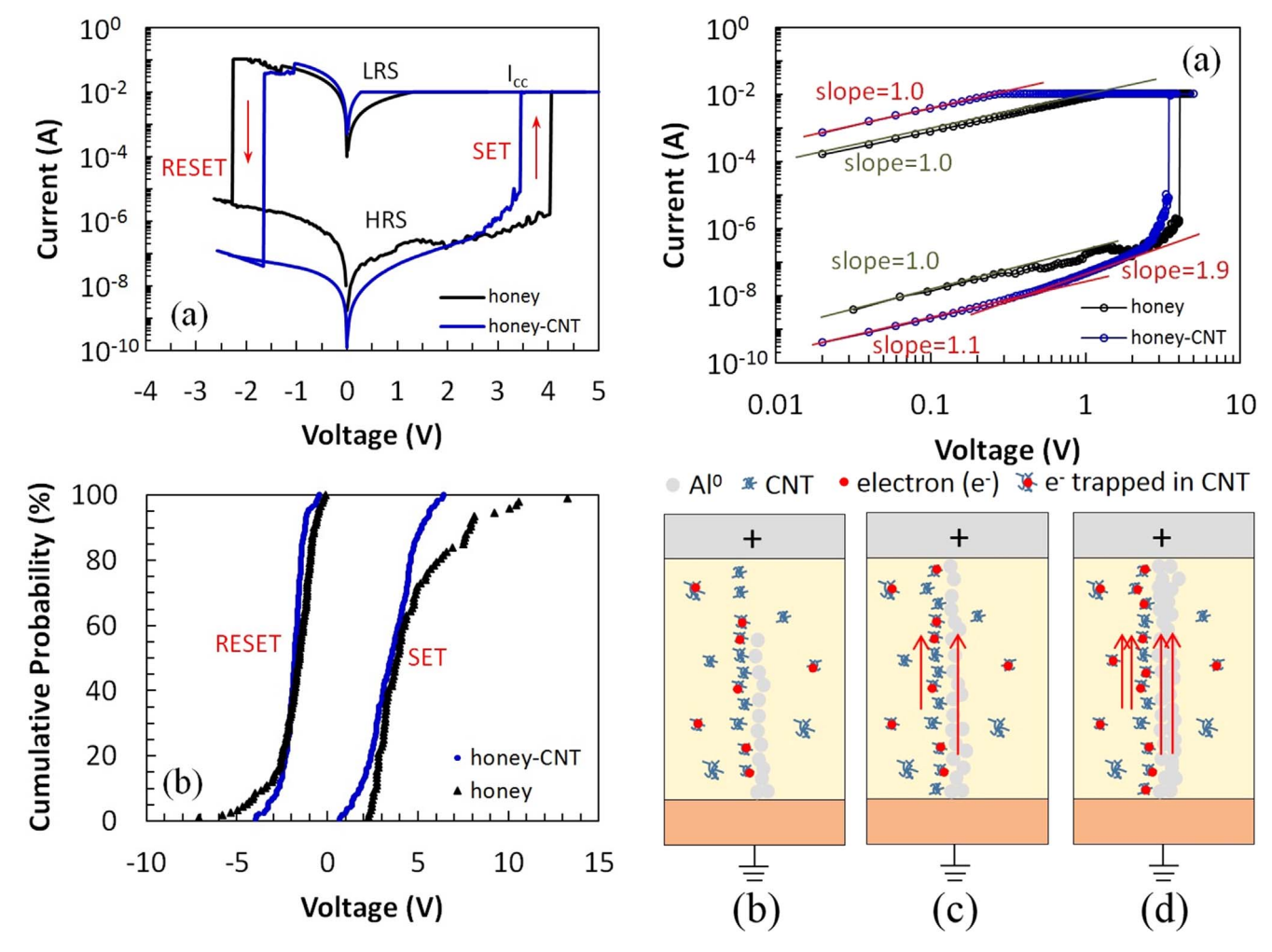


Figure 3 (a) Typical bipolar switching of pure honey and honey-CNT RSMs. $I_{\rm CC}$: current compliance. (b) Endurance of $V_{\rm set}$ and $V_{\rm reset}$ in 200 switching cycles.

Figure 4. (a) Replot of figure 3(a) in positive voltage sweep in loglog scale with the slope of each I-V curve. Schematic of resistive switching evolution in honey-CNT RSM in HRS when voltage is (b) low, (c) approaching $V_{\rm set}$, and (d) equal to $V_{\rm set}$.

metallic filaments is bridging between bottom and top electrodes at V_{set} [figure 4(d)]. During the formation of metallic filaments, bundles of CNTs can be aligned along the filaments and assisting in bridging the conduction of electrons. For honey-CNT film in HRS, the slope also closed to unity in low voltage range but increased to 1.9 when voltage approached $V_{
m set}$. This slope value indicated that the current conduction is governed by the space charge limited conduction (SCLC) model [27] due to the traps in the honey-CNT film. This observation is consistent with the result from CNT embedded egg albumen film [24]. The traps can be attributed to CNTs which attract electrons strongly. During the filament formation under low voltages, electrons were captured by CNT agglomerations as shown in figure 4(b) and could not escape due to low energy and mobility. When the voltage approached V_{set} , higher energy and mobility allow the filled electrons to escape from trap centers and transport along CNT agglomerations as well as filaments between the top and bottom electrode as shown in figure 4(c), resulting in an increased current slope from 1 to 1.9. At V_{set} , more conductive filaments were formed and more electrons transported along CNTs and filaments as shown in figure 4(d), with current increasing abruptly to compliance and device transiting to LRS.

The switching speed is another important resistive switching characteristic. The circuit diagram for this test has been reported before [18]. Figures 5(a)–(c) shows the transient response of honey-CNT RSM in SET and RESET process. The time delay between input and output voltage pulses determines the SET time for device to switch on (transit from HRS to LRS), while the pulse width of the output voltage pulse determines the RESET time for device to switch off (transit from LRS to HRS). The SET and RESET times derived from transient response were 30 ns and 200 ns, respectively. This switching speed is faster than previously reported pure honey RSM [18] and comparable to other reported RSMs based on metal oxide or natural materials such as SiO₂ [28] and pectin [29].

Data retention refers to the ability of a memory device to retain its data state over a long period of time [30]. The data state is demonstrated by HRS and LRS currents in the retention test. In general, it is expected that a good nonvolatile

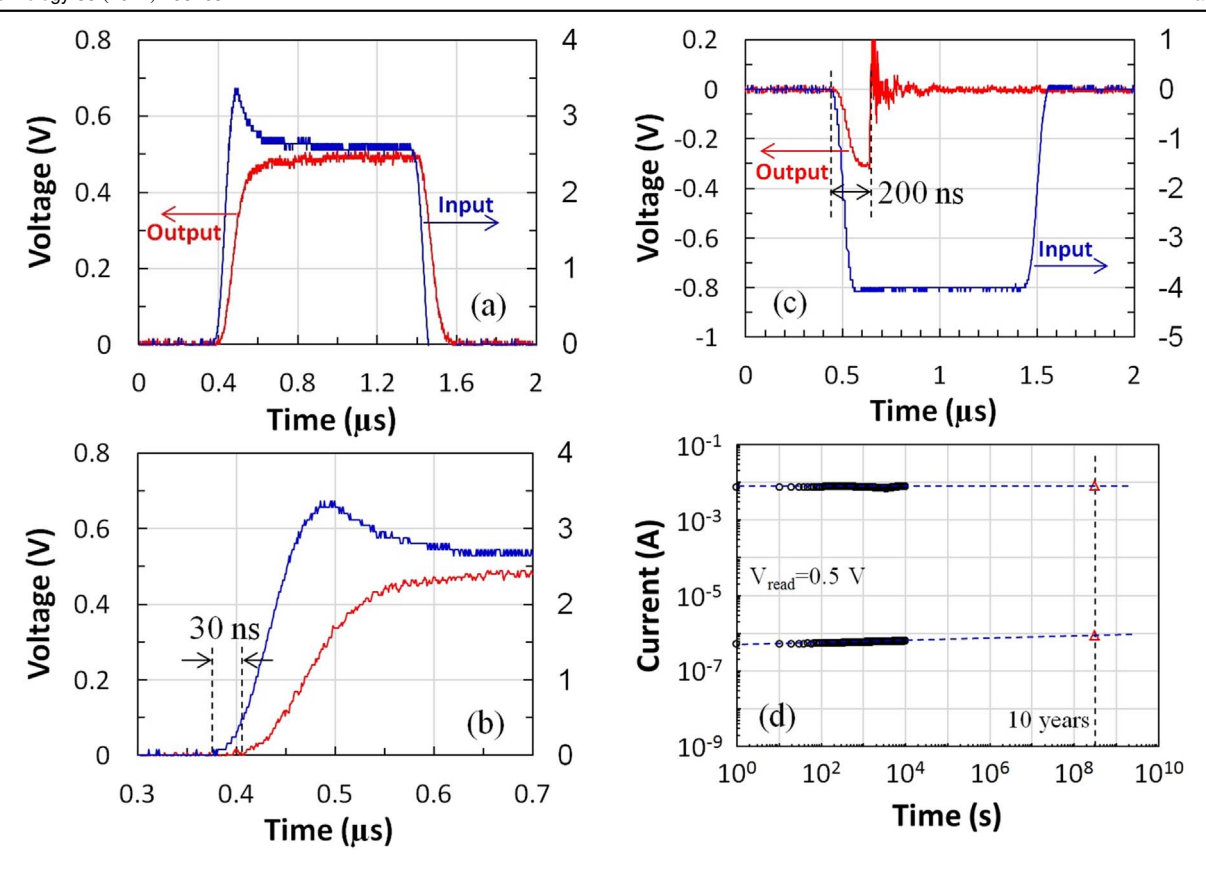


Figure 5. Transient response in (a), (b) SET and (c) RESET process with honey-CNT memory triggered by input voltage pulse (blue). The SET and RESET time was extracted from the delay time and output voltage pulse (red) width, respectively. (d) Data retention characteristics for both LRS and HRS of the honey-CNT RSM tested at an interval of 10 s for 10⁴ s. The retention was extrapolated to 10 years.

memory device should be capable of storing data for at least 10 years [30–32], but such test duration is not practical in the research laboratory. The widely accepted method is to test the device continuously for 10⁴ s, with the LRS and HRS current values recorded and extended to 10 years for a projection of the data retention life. If HRS and LRS currents are stable without significant degradation within the whole 10⁴ s test duration, and the extrapolated current values at the 10 year time still maintain the initial ON/OFF ratio, then it can be claimed that the device has a good retention property and a potential for data retention life of 10 years. In this study, data retention tests were also performed for 10⁴ s under ambient and room temperature to test the data storage stability of honey-CNT RSM. The device was switched to LRS by the SET process, then the voltage was fixed at the read voltage $V_{\rm read} = 0.5 \text{ V}$ and LRS current values were recorded every 10 s. As shown in figure 5(d), LRS current was stable at 7.5 mA without any noticeable degradation for the whole 10⁴ s test duration. After LRS test, the RESET process was applied to switch the device back to HRS. The voltage was fixed at $V_{\rm read} = 0.5 \text{ V}$ with HRS current values recorded every 10 s again. Test results showed that the HRS current was also relatively stable and only increased gradually from 500 to 650 nA over the whole 10⁴ s. Afterward, both LRS and HRS currents in figure 5(d) were projected for a 10 year horizon of operation. It is shown that the ON/OFF ratio of 1×10^4 was still maintained, indicating that honey-CNT RSM has an excellent data retention ability.

Compared with previously reported pure honey-RSM devices [17–20] and other natural organic materials based RSM devices [22–24] embedded with nanomaterials such as CNTs and nanoparticles, this study shows that the incorporation of CNTs in honey-RSM devices can lower the HRS leakage current, increase the ON/OFF current ratio, and reduce SET and RESET time response and increase switching speed, which are desirable for nonvolatile memory. This study established a useful practice for fabrication of RSM devices based on honey and can be extended to other natural organic materials.

Conclusion

CNT embedded honey film as a resistive switching material was studied and compared with pure honey film. CNT agglomerations are presented in the honey film as demonstrated by morphology characterization by AFM and optical surface profiler. This is due to the inefficient dispersion of CNTs in honey-water solution. Honey-CNT film and pure honey film were fabricated in RSM device structures. Both RSM devices exhibited bipolar resistive switching, but devices with honey-CNT film showed a better endurance stability with less deviation in both $V_{\rm SET}$ and $V_{\rm RESET}$ for 200 cycles

and faster switching speed of 30 ns and 200 ns for SET and RESET times, respectively. The retention of honey-CNT device is expected to be stable up to 10 years. The current conduction mechanism of the CNT-honey film is attributed to conductive filaments following Ohm's law in the whole LRS and only at low voltages in HRS. At high voltages in HRS, the current conduction was governed by SCLC due to the transport of electrons along CNT traps as well as conductive filaments.

Acknowledgments

Feng Zhao acknowledges the support from National Science Foundation, United States (ECCS-2104976). Zhigang Xiao acknowledges the support from National Science Foundation, United States (ECCS-2105388). Research carried out in part at the Center for Functional Nanomaterials, Brookhaven National Laboratory, which is supported by the U.S. Department of Energy, Office of Basic Energy Sciences, under Contract No. DE-SC00112704.

Data availability statement

The data that support the findings of this study are available upon reasonable request from the authors.

ORCID iDs

Kuan Yew Cheong https://orcid.org/0000-0001-8049-0297

Feng Zhao https://orcid.org/0000-0001-9350-6497

References

- [1] Li Y, Wang Z, Midya R, Xia Q and Joshua Yang J 2018 Review of memristor devices in neuromorphic computing: materials sciences and device challenges *J. Phys. D: Appl. Phys.* **51** 503002
- [2] Smith J D, Hill A J, Reeder L E, Franke B C, Lehoucq R B, Parekh O, Severa W and Aimone J B 2022 Neuromorphic scaling advantages for energy-efficient random walk computations *Nat. Electron.* 52 102–12
- [3] Shi T, Wang R, Wu Z H, Sun Y Z, An J J and Liu Q 2021 A review of resistive switching devices: performance improvement, characterization, and applications *Small Struct.* 2 2000109
- [4] Zahoor F, Zainal T Z A and Khanday F 2020 A resistive random access memory (RRAM): an overview of materials, switching mechanism, performance, multilevel cell storage, modeling, and applications *Nanoscale Res. Lett.* 15 90
- [5] Bazzi H, Harb A, Aziza H and Moreau M 2020 Non-volatile SRAM memory cells based on ReRAM technology SN Appl. Sci. 2 1485
- [6] John R A et al 2020 Self healable neuromorphic memtransistor elements for decentralized sensory signal processing in robotics Nat. Commun. 11 1–12

- [7] Yao P, Wu H, Gao B, Tang J S, Zhang Q T, Zhang W Q, Yang J J and Qian H 2020 Fully hardware-implemented memristor convolutional neural network *Nature* 577 641–6
- [8] Tang J S et al 2019 Bridging biological and artificial neural networks with emerging neuromorphic devices: fundamentals, progress, and challenges Nature 31 1902761
- [9] Chang Y F, Zhou F, Fowler B W, Chen Y C, Hsieh cc, Guckert L, Swartzlander E E and Lee J C 2017 Memcomputing (memristor + computing) in intrinsic SiOx-based resistive switching memory: arithmetic operations for logic applications *IEEE Trans. Electron Devices* 64 2977–83
- [10] Pi S, Ghadiri-Sadrabadi M, Bardin J and Xia Q F 2015 Nanoscale memristive radiofrequency switches nature Communications 6 7519
- [11] Lin Q, Hao S, Hu W, Wang M, Zang Z, Zhu L, Du J and Tang X 2019 Human hair keratin for physically transient resistive switching memory devices J. Mater. Chem. C 7 3315–21
- [12] Sung S, Park J H, Wu C and Kim T W 2020 Biosynaptic devices based on chicken egg albumen:graphene quantum dot nanocomposites Sci. Rep. 10 1–8 101
- [13] Liu S, Dong S, Wang X, Shi L, Xu H, Huang S and Luo J 2020 Flexible and fully biodegradable resistance random access memory based on a gelatin dielectric *Nanotechnology* 31 255204
- [14] Xing Y, Sueoka B, Cheong K Y and Zhao F 2021 Nonvolatile resistive switching memory based on monosaccharide fructose film Appl. Phys. Lett. 119 163302
- [15] Arshad N, Irshad M S, Abbasi M S, Ur Rehman S, Ahmed I, Javed M Q, Ahmad S, Sharaf M and Al Firdausi M D 2021 Green thin film for stable electrical switching in a low-cost washable memory device: proof of concept RSC Adv. 11 4327–38
- [16] Dlamini Z W, Vallabhapurapu S, Wu S, Mahule T S, Srivivasan A and Vallabhapurapu V S 2022 Resistive switching memory based on chitosan/polyvinylpyrrolidone blend as active layers *Solid State Commun.* 345 114677
- [17] Sivkov A A, Xing Y, Cheong K Y, Zeng X and Zhao F 2020 Investigation of honey thin film as a resistive switching material for nonvolatile memories *Mater. Lett.* 271 127796
- [18] Sueoka B and Zhao F 2022 Memristive synaptic device based on a natural organic material—honey for spiking neural network in biodegradable neuromorphic systems J. Phys. D: Appl. Phys. 55 225105
- [19] Sueoka B, Cheong K Y and Zhao F 2022 Natural biomaterial honey-based resistive switching device for artificial synapse in neuromorphic systems Appl. Phys. Lett. 120 083301
- [20] Sueoka B, Cheong K Y and Zhao F 2022 Study of synaptic properties of honey thin film for neuromorphic systems *Mater. Lett.* 308 131169
- [21] Da Silva P M, Gauche C, Gonzaga L V, Costa A C O and Fett R 2016 Honey: chemical composition, stability and authenticity Food Chem. 196 309–23
- [22] Do H H H, Le T M and Pham N K 2021 The resistive switching behavior of Al/chitosan-graphene oxide/FTO structure J. Nanomater. 2021 5565169
- [23] Guo B, Sun B, Hou W, Chen Y, Zhu S, Mao S, Zheng L, Lei M, Li B and Fu G 2019 A sustainable resistive switching memory device based on organic keratin extracted from hair RSC Adv. 9 12436–40
- [24] Wang L, Yang T and Wen D 2021 Tunable multilevel data storage bioresistive random access memory device based on egg albumen and carbon nanotubes *Nanomaterials* 11 2085
- [25] Cheong K Y, Tayeb I A, Zhao F and Abdullah J M 2021 Review on resistive switching mechanisms of bio-organic thin film for non-volatile memory application *Nanotechnol. Rev.* 10 680–709

- [26] Wang L, Zhu H and Wen D 2021 Bioresistive random-access memory with gold nanoparticles that generate the coulomb blocking effect can realize multilevel data storage and synapse simulation *J. Phys. Chem. Lett.* 12 8956–62
- [27] Lampert M A 1956 Simplified theory of space-charge-limited currents in an Insulator with traps *Phys. Rev.* 103 1648
- [28] Gao S *et al* 2014 Resistive switching and conductance quantization in Ag/SiO₂/indium tin oxide resistive memories *Appl. Phys. Lett.* **105** 063504
- [29] Xu J, Zhao X, Wang Z, Xu H, Hu J, Ma J and Liu Y 2019 Biodegradable natural pectin-based flexible multilevel resistive switching memory for transient electronics *Small* 15 1803970
- [30] Niset M and Kuhn P 2005 Typical data retention for nonvolatile memory Freescale Semiconductor Engineering Bulletin (https://nxp.com/docs/en/engineering-bulletin/ EB618.pdf)
- [31] Hirsch K 2004 Manufacturing effects on data retention of nonvolatile memory devices (http://circuitsassembly.com/ cms/images/stories/pdf/0411/0411dataio.pdf)
- [32] Endurance and data retention characterization of Infineon flash memory, Infineon Application Note 217979 2021 (https://infineon.com/dgdl/Infineon-AN217979_Endurance_and_Data_Retention_Characterization_of_Infineon_Flash_Memory-ApplicationNotes-v03_00-EN.pdf?fileId=8ac78c8c7cdc391c017d0d30d6b064f5)